**Revision 1**

**Supplementary to "Elastic geobarometry: how to work with residual inclusion strains and pressures"**

Mattia Gilio[1], Ross J. Angel[2] and Matteo Alvaro[1]

[1]Department of Earth and Environmental Sciences, via Ferrata, 4, University of Pavia, Pavia, Italy

[2]IGG-CNR, Via G. Gradenigo, 6, Padova, Italy

**The hydrostatic stress line of quartz: calculation methods and implications**

As a quartz crystal is compressed (or expanded) under hydrostatic stress conditions, it will develop deviatoric strains according to its elastic response. This change of strain with pressure can be visualized as a line in a strain graph. **Figure S1** is a $\varepsilon_1+\varepsilon_2$ vs $\varepsilon_3$ graph showing the hydrostatic stress lines of quartz, obtained with different methods. The yellow dashed line was obtained using the axial equation of state (EoS; Alvaro et al., 2020; Scheidl et al., 2016), while the blue and green line using the 1 bar adiabatic (Wang et al., 2015) and isothermal (Mazzucchelli et al., 2020) elastic tensors of quartz, respectively. The graph also includes the lines of equal $P_{inc}^{464}$ and $P_{inc}$ (in red and black, respectively) calculated as for **Figure 1** in the paper. The hydrostatic inclusion pressure ($P_{inc}^{464}$; red lines in **Figure S1**) was calculated by converting the strain into Raman shift using the Grüneisen tensor $\Delta\omega_{464} = -[\gamma_1^{464}(\varepsilon_1 + \varepsilon_2) + \gamma_3^{464}\varepsilon_3] * \omega_{464}$, (Angel et al., 2019), where $\gamma_1^{464}$ and $\gamma_3^{464}$ are the Grüneisen tensor components for mode $\omega_{464}$, calculated *ab-initio* by Murri et al. (2018). The $P_{inc}^{464}$ was then calculated using the hydrostatic calibration $P_{inc}^{464} = \left(0.00029 * \Delta\omega_{464}{}^2 + 0.118 * \Delta\omega_{464}\right) GPa$ by Morana et al. (2020).

The line of hydrostatic stress calculated with the isothermal (green dashed line) and adiabatic (blue dashed line) elastic tensors are very similar because the two tensors have the same component values within their uncertainties. The green circles in **Figure S1** represent the hydrostatic stress at that point. The hydrostatic line in blue does not have such circles because they fall exactly at the intercept between the line itself and the lines of equal $P_{inc}$ (in black) as they were both calculated with the same tensor. We omitted these symbols so as to not to overburden the graph.

The hydrostatic line calculated from the measured variation of the unit cell parameters with pressure (yellow dashed line; Scheidl et al., 2016) is subparallel to the one obtained with the elastic tensor (in blue) in the pressure range in the graph (0-2.5 GPa). The yellow line is not a straight line because the anisotropy of compressibility of quartz changes with increasing pressure, so its difference with the line calculated with the room-pressure elastic

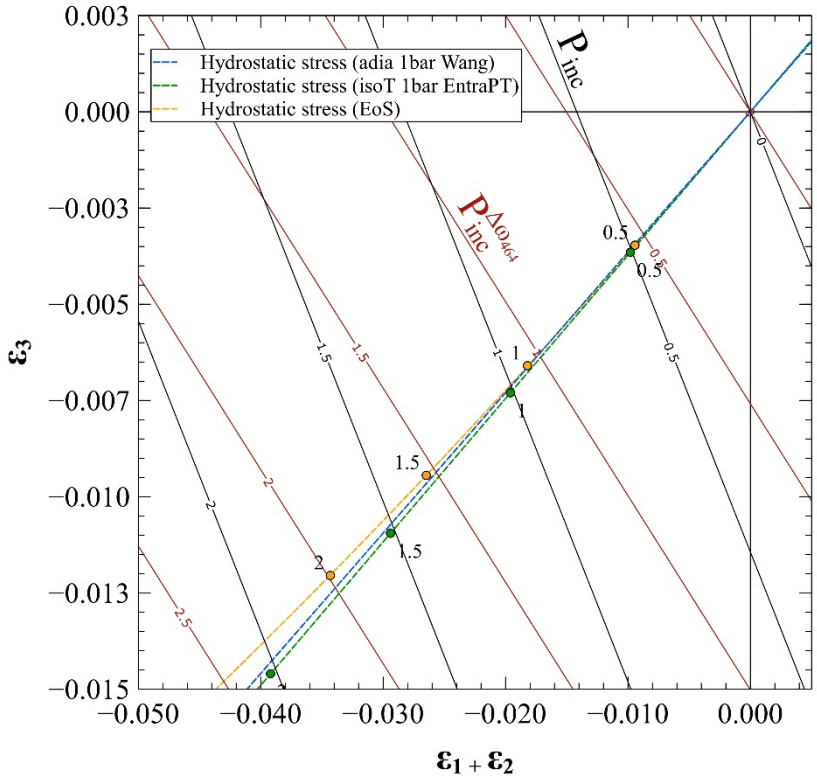


*Figure S1 - Graph of $\varepsilon_1+\varepsilon_2$ vs. $\varepsilon_3$ displaying the lines of mean normal stress ($P_{inc}$) of quartz calculated from the stiffness tensor (in black), and the lines of inclusion pressure calculated using the hydrostatic calibration ($P_{inc}^{464}$) by Morana et al. (2020). The yellow dashed line is the hydrostatic stress of quartz calculated with the quartz EoS (Scheidl et al., 2016). The green and the blue dashed line are the hydrostatic stress lines calculated with the 1 bar isothermal (Mazzucchelli et al., 2020) and adiabatic (Wang et al., 2015) elastic tensor, respectively.*

moduli (which is linear) increases exponentially for higher pressures. This means that, for pressures < 2.5 GPa, the differential strain ($\frac{\varepsilon_1+\varepsilon_2}{\varepsilon_3}$) remains roughly constant for hydrostatic stress, regardless of the calculation method (elastic tensor at 1bar vs. EoS). However, the absolute value of pressure for discrete points along the hydrostatic line changes (yellow circles in Figure 1). For example, the yellow circles almost overlap with the red and black lines ($P_{inc}^{464}$ and $P_{inc}$, respectively) at 0.5 GPa. Instead, at higher $P_{inc}$ (e.g., 1.0, 1.5, and 2.0 GPa) the yellow circles lie only on the red lines of $P_{inc}^{464}$ at of the same pressure. This means that, for low inclusion pressures, the difference in strain for the same hydrostatic pressure is relatively small between strains calculated with the EoS and with the elasticity tensor. However, the higher the hydrostatic pressure, the larger is the difference in strain between these two methods. Furthermore, the lines of equal $P_{inc}^{464}$ (red lines) cross the line of hydrostatic stress calculated with the EoS at almost the same pressures (the red lines and the yellow-dashed line cross at, or near, the yellow circles). This is because both the EoS and the lines of equal $P_{inc}^{464}$ derive from hydrostatic measurements. The predictions by the elastic tensor at 1 bar are different from results from hydrostatic DAC experiments because

the elastic tensor is valid only for infinitesimal strains at the reference pressure (1 bar) and does not account for either the stiffening nor change in elastic anisotropy of quartz as pressure and strains are increased. So, the only strictly valid line of equal $P_{inc}$ in black in the figure is the one at 0 GPa. However, the elastic tensor allows one to explore the behaviour of quartz inclusions subjected to differential strain. Since quartz inclusions in garnet from both natural and experimental samples are generally under a non-hydrostatic stress, we have to assume that the elastic tensor is valid for the ranges of strains ($-0.05 < \varepsilon_1+\varepsilon_2 < 0.03$ and $-0.02 < \varepsilon_3 < 0.02$).

## References

Alvaro, M., Mazzucchelli, M., Angel, R., Murri, M., Campomenosi, N., Scambelluri, M., Nestola, F., Korsakov, A., Tomilenko, A., and Marone, F. (2020) Fossil subduction recorded by quartz from the coesite stability field. Geology, 48(1), 24-28.

Angel, R.J., Murri, M., Mihailova, B., and Alvaro, M. (2019) Stress, strain and Raman shifts. Zeitschrift für Kristallographie-Crystalline Materials, 234(2), 129-140.

Mazzucchelli, M.L., Angel, R.J., and Alvaro, M. (2020) EntraPT: an online platform for elastic geothermobarometry. American Mineralogist.

Morana, M., Mihailova, B., Angel, R.J., and Alvaro, M. (2020) Quartz metastability at high pressure: what new can we learn from polarized Raman spectroscopy? Physics and Chemistry of Minerals, 47(8), 1-9.

Murri, M., Mazzucchelli, M.L., Campomenosi, N., Korsakov, A.V., Prencipe, M., Mihailova, B.D., Scambelluri, M., Angel, R.J., and Alvaro, M. (2018) Raman elastic geobarometry for anisotropic mineral inclusions. American Mineralogist, 103(11), 1869-1872.

Scheidl, K.S., Kurnosov, A., Trots, D.M., Boffa Ballaran, T., Angel, R.J., and Miletich, R. (2016) Extending the single-crystal quartz pressure gauge up to hydrostatic pressure of 19 GPa. Journal of Applied Crystallography, 49(6), 2129-2137.

Wang, J., Mao, Z., Jiang, F., and Duffy, T.S. (2015) Elasticity of single-crystal quartz to 10 GPa. Physics and Chemistry of Minerals, 42(3), 203-212.